Uplink Channel Estimation and Equalization in NB-IoT System

Vincent Savaux, Hamidou Dembélé, Matthieu Kanj

Uplink Channel Estimation and Equalization in NB-IoT System

Vincent Savaux, Hamidou Dembélé, and Matthieu Kanj
b<>com, Rennes, France
Email: {vincent.savaux,hamidou.dembele,matthieu.kanj}@b-com.com

***Abstract*—This paper deals with channel estimation and equalization, as well as noise variance estimation in uplink narrowband-internet of things (NB-IoT) system. Different techniques are studied in the context of NB-IoT, such as least square (LS) and linear minimum mean square error (LMMSE) for channel estimation, and zero forcing (ZF) and MMSE for equalization. It is shown that a low-complexity application of MMSE-based methods is made possible in NB-IoT by taking advantage of the small number of subcarriers. Furthermore, a noise variance estimator is suggested based on the combination of two successive observations of pilots, assuming slowly varying channel. We also prove that the proposed estimator is efficient, and confirm by simulations that both LMMSE channel estimator and MMSE equalizer can use the estimated noise variance instead of the exact value without loss of performance.**

I. Introduction

NarrowBand-internet of things (NB-IoT) system is a newly introduced 3rd generation partnership project (3GPP) standard designed to provide connectivity for a wide range of cellular devices and enable new internet of things services [1]. It was introduced to cope with the growing market of machine-type communication where the usage of connected devices will exponentially increase due to the expansion of applications proposed for individuals and industries. At the same time, this new system was conceived to provide IoT services through the legacy wide-area cellular networks such as LTE. To this end, the NB-IoT system was inherited from Long Term Evolution (LTE) system (see overviews about NB-IoT in [2]–[5]). It is designed to be easily integrated in LTE networks to provide fast and flexible deployment. However, it was adapted to take into account the constraints related to IoT devices. In particular, very good indoor coverage, support of huge number of connected devices, low device cost, low computation capacity and low power consumption.

The design of NB-IoT system is based on the orthogonal frequency division multiplexing (OFDM) modulation scheme. The NB-IoT downlink signal only occupies 12 subcarriers of 15 kHz each, which corresponds to one resource block (RB) in LTE. For uplink transmission, the single-carrier frequency division multiple access (SC-FDMA) modulation scheme is also kept from LTE. Moreover, the same framing structure is kept from LTE but with difference in channels and signals mapping. Therefore, the NB-IoT system has a frame duration of 10 ms and comprises 10 sub-frames of 1 ms each, which corresponds to 20 slots of 0.5 ms. However, there is no extended cyclic prefix option and thus each slot is strictly composed of 7 OFDM symbols.

In this respect, the NB-IoT system inherited almost the same issues in terms of signal processing due to the reuse of the same transmission techniques. However, the additional challenge here is to achieve a deep indoor coverage especially when dealing with the NB-IoT UE modules that are far from the base station. Moreover, this challenge is amplified since SC-FDMA is sensitive to residual errors of channel estimation and equalization, since the decoding step inherent to SC-FDMA spreads errors over all the subcarriers.

To reveal this challenge, efficient algorithms are required for the uplink channel estimation accuracy. In the literature, several channel estimation and equalization techniques were proposed to improve the reliability of uplink transmission in LTE [6]. Most of techniques are based on the use of demodulation reference signal (DMRS) also called pilots. Moreover, these techniques were extensively studied for multicarrier systems with high bandwidth such as LTE, but not much considered for narrow-band system.

In this work, we consider different channel estimation and equalization techniques that we adapt to NB-IoT system. Among others, the most commonly used are: least square (LS) and linear minimum mean square error (LMMSE) for channel estimation, and zero forcing (ZF) and MMSE for equalization. Generally, LS and ZF techniques are simple but are sensitive to the noise, whereas LMMSE and MMSE methods are more complex but show better performance. In addition to their complexity, MMSE-based methods require the knowledge of the noise variance, which is *a priori* unknown. These two drawbacks limit the practical application of MMSE-based estimation and equalization techniques.

We suggest to take advantage of NB-IoT features to make MMSE-based techniques applicable in practice to NB-IoT system. In this respect, we show that the low number of subcarriers leads to a reduction in complexity. Moreover, the environment is supposed to be slowly varying, which is consistent with the commercial applications

ISBN 978-3-903176-18-8

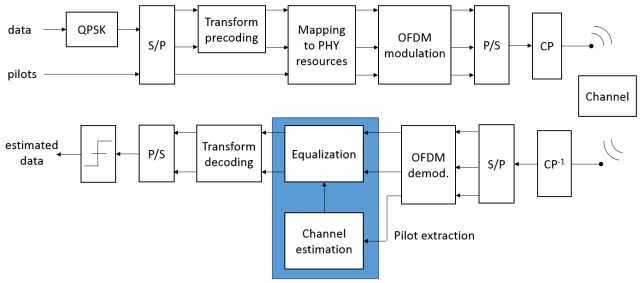

Fig. 1. Simplified block diagram of TX/RX chain. TX corresponds to UE side, RX to evolved node B (eNB) side.

of NB-IoT. Thus, we can combine the observations of different received pilots to reduce the noise disruptions, and to estimate the noise variance, which is required in MMSE-based methods. Finally, the performance of the different estimators are theoretically analyzed and compared through simulations, and the assumptions on the channel model are discussed.

The rest of this paper is organized as follow. In section II, we present the model of the uplink NB-IoT signal and describe the considered estimation and equalization techniques. In section III, we show how to adapt these techniques to the characteristics of NB-IoT signal. Section IV is dedicated to simulation results. In section V , a complexity analysis is presented to compare the considered techniques. Conclusions and future works are presented in section VI.

Notation: The scalars are written in normal font X, vectors in boldface $\mathbf{X}$, and matrices in underlined boldface $\underline{\mathbf{X}}$. The superscripts $(.)^{-1}$, $(.)^T$, and $(.)^H$ denote the inverse, the transpose, and the Hermitian (conjugate) transpose operators, respectively. Furthermore, $\mathbb{E}\{.\}$ is the mathematical expectation, ln(.) the natural logarithm, and $\|.\|$ and $|.|$ the Euclidian norm and the modulus, respectively.

II. System Model

This section is dedicated to the description of the NB-IoT uplink signal model, as well as usual channel estimation and equalization techniques in multicarrier systems such as LS and LMMSE (for estimation), and ZF and MMSE (for equalization). Both single-carrier and multicarrier configuration modes are allowed for uplink transmission in 3GPP TS 36.211 [1]. However, we focus here on multicarrier mode since the aim of this paper is to deal with SC-FDMA modulation. Furthermore, the single-carrier mode involves almost trivial processes at the receiver, which can be simply deduced from the hereby presented results.

A. Uplink Received Signal Model

The general transmission/reception (TX/RX) chain in uplink NB-IoT is depicted in Fig. 1, where channel estimation and equalization blocks are highlighted. According to [1], and in the same way as in LTE [7], all the subcarriers of the fourth symbol of each uplink slot (a slot 1 composed of 7 consecutive OFDM symbols) are pilot elements. Therefore, in order to perform per-subcarrier estimation, these pilot elements are not precoded (contrarily to data elements that are precoded in SC-FDMA). Thus, the $M\times 1$ received signal vector in frequency domain (*i.e.* at the output of the OFDM demodulation block), denoted by $\mathbf{Y}_n$, can be expressed as

$$\mathbf{Y}_n = \begin{cases} \underline{\mathbf{H}}_n\mathbf{X}_n + \mathbf{W}_n, & \text{if } n = 3 \\ \underline{\mathbf{H}}_n\underline{\mathbf{F}}\mathbf{X}_n + \mathbf{W}_n, & \text{if } n \neq 3 \end{cases}, \tag{1}$$

where n is the index of the symbol within a slot ($n = 0, 1, .., 6$). We denote by $m = 0, 1, .., M-1$ the subcarrier index, by $\mathbf{X}_n = [X_{n,0}, .., X_{n,m}, .., X_{n,M-1}]^T$ the $M \times 1$ complex vectors of the transmitted signal (precoded data or pilots) and by $\mathbf{W}_n = [W_{n,0}, .., W_{n,m}, .., W_{n,M-1}]^T$ the additive white Gaussian noise (AWGN). Note that $W_{n,m} \sim \mathbb{C}\mathcal{N}(0, \sigma_W^2)$ for any $m = 0, 1, .., M-1$, $\underline{\mathbf{H}}_n$ is the $M \times M$ diagonal matrix containing the complex frequency response of the channel, and $\underline{\mathbf{F}}$ is the $M \times M$ DFT precoding matrix.

For clarity purpose, we define the variable $\mathbf{Z}_n = \underline{\mathbf{F}}\mathbf{X}_n$ and we use the subscript p to highlight pilot symbols, *i.e.* $\mathbf{Y}_p = \underline{\mathbf{H}}_p\mathbf{X}_p + \mathbf{W}_p$ if $n = p = 3$. Moreover, since we focus on channel estimation and equalization, we consider the following assumptions in the remaining of the paper:

- The maximum delay spread of the channel is shorter than the CP, in such a way that no intersymbol interference (ISI) occurs. Furthermore, it is supposed to be quasi-static, *i.e.* static over at least one slot (this will be further discussed). Thus, channel equalizer uses the same estimate over at least one slot.
- Time and frequency synchronization is perfect, then no intercarrier interference (ICI) occurs.

Based on these assumptions, we describe in the next sub-section the usual channel estimation and equalization techniques considered in this paper.

B. Channel Estimation and Equalization

1) Channel Estimation: As a prerequisite to channel estimation, it is noteworthy that $\mathbf{Y}_p$ can be rewritten as $\mathbf{Y}_p = \underline{\mathbf{X}}_p\mathbf{H}_p + \mathbf{W}_p$, where $\underline{\mathbf{X}}_p$ is the diagonal matrix containing the elements of $\mathbf{X}_p$, and $\mathbf{H}_p$ is the vector containing the frequency response of the channel. From this, we derive the expression of the channel estimate using LS and LMMSE methods, such as presented in [8]–[11].

a) Least Square (LS): LS method is based on the minimization of the cost function $J_{LS} = \|\mathbf{Y}_p - \underline{\mathbf{X}}_p\mathbf{H}_p\|^2$, which yields to:

$$\hat{\mathbf{H}}_p^{LS} = \underline{\mathbf{X}}_p^{-1}\mathbf{Y}_p = \mathbf{H}_p + \underline{\mathbf{X}}_p^{-1}\mathbf{W}_p. \tag{2}$$

Note that in the case of preamble (or midamble) pilot scheme, (*i.e.* when a whole OFDM symbol is composed

of pilots such as in uplink NB-IoT) the LS estimate in (2) can also be obtained by the maximum likelihood (ML) estimator. In fact, it is known that the maximization of the likelihood function $L = C.exp(-\frac{\|\mathbf{Y}_p - \underline{\mathbf{X}}_p \mathbf{H}_p\|^2}{2\sigma_W^2}) = C.exp(-\frac{\|J_{LS}\|^2}{2\sigma_W^2})$ is strictly equivalent the minimization of J_{LS}, since the function e^{-x^2} reaches its maximum when x reaches its minimum. This assumption does not hold anymore when pilots and data are multiplexed in an OFDM symbol. The LS estimator is easy to implement, but it is sensitive to noise, which is highlighted by the term $\underline{\mathbf{X}}_p^{-1}\mathbf{W}_p$ in (2).

b) Linear Minimum Mean Square Error (LMMSE): LMMSE method is based on the minimization of the cost function $J_{LMMSE} = \|\mathbf{H}_p - \underline{\mathbf{D}}\mathbf{Y}_p\|^2$, where $\underline{\mathbf{D}}$ is a matrix whose expression is given below. The minimization of J_{LMMSE} with respect to $\underline{\mathbf{D}}$ finally leads to (see [11] for details):

$$\begin{aligned}\hat{\mathbf{H}}_p^{LMMSE} &= \overbrace{\underline{\mathbf{R}}_H(\underline{\mathbf{R}}_H + (\underline{\mathbf{X}}_p\underline{\mathbf{X}}_p^H)^{-1}\sigma_W^2)^{-1}\underline{\mathbf{X}}_p^{-1}}^{\underline{\mathbf{D}}}\mathbf{Y}_p \\ &= \underline{\mathbf{R}}_H(\underline{\mathbf{R}}_H + (\underline{\mathbf{X}}_p\underline{\mathbf{X}}_p^H)^{-1}\sigma_W^2)^{-1}\hat{\mathbf{H}}_p^{LS}, \end{aligned} \quad (3)$$

where $\underline{\mathbf{R}}_H$ is the channel covariance matrix. The matrix $\underline{\mathbf{R}}_H(\underline{\mathbf{R}}_H + (\underline{\mathbf{X}}_p\underline{\mathbf{X}}_p^H)^{-1}\sigma_W^2)^{-1}$ acts like a smoothing filter on $\hat{\mathbf{H}}_p^{LS}$, leading to a reduction of noise disruption in the estimate $\hat{\mathbf{H}}_p^{LMMSE}$.

In fact, the mean square error (MSE) analysis as in [12], [13] has proved that LMMSE estimator shows better performance than LS estimator. This feature will also be shown in Section IV. We can notice from (3) that LMMSE estimator involves matrix inversion and multiplication, which is much more complex than LS estimation. In addition, it requires the prior knowledge of $\underline{\mathbf{R}}_H$ and σ_W^2, which limits its practical application.

In order to overcome this drawback, it has been proposed by Edfors *et al.* in [12], [14] to substitute the exact channel covariance matrix $\underline{\mathbf{R}}_H$ by an approximated matrix $\underline{\tilde{\mathbf{R}}}_H$, whose eigenvalues λ_m, with $m = 0, 1, .., M-1$, are set in advance. It remains that σ_W^2 is still an unknown parameter. This is the reason why we propose an estimator of σ_W^2 in Section III. Moreover, the complexity of LMMSE will be discussed in Section V.

2) Channel Equalization: The goal of channel equalization is to invert the channel in order to estimate the symbols $\mathbf{Z}_n$. In fact, since we are considering a multicarrier system, we can use a per-subcarrier equalizer. In this respect, we define the $M \times M$ diagonal equalization matrix $\mathbf{Q}$, such that the estimated symbols can be expressed as $\hat{\mathbf{Z}}_n = \underline{\mathbf{Q}}\mathbf{Y}_n$.

a) Zero Forcing (ZF): The ZF equalizer is defined as follows:

$$\underline{\mathbf{Q}} = \underline{\mathbf{H}}_p^{-1} \approx \hat{\underline{\mathbf{H}}}_p^{-1}, \quad (4)$$

where $\hat{\underline{\mathbf{H}}}_p$ is the $M \times M$ diagonal matrix that contains the estimated channel values. This is the simplest equalization technique, but the gain of the equalizer may be high at some subcarriers if $H_{p,m}$ is weak, which amplifies the noise. In fact, the exact frequency response should not be available at the receiver. Thus, in practice, the exact frequency response is substituted by the estimated one, such as suggested in (4).

b) Minimum Mean Square Error (MMSE): The aim of MMSE equalizer is to find the diagonal matrix $\underline{\mathbf{Q}}$ that minimizes the error function $e = \mathbb{E}\{\|\mathbf{X}_n - \hat{\mathbf{X}}_n\|^2\}$, where $\mathbb{E}\{.\}$ is the mathematical expectation, and $\hat{\mathbf{X}}_n = \underline{\mathbf{Q}}\mathbf{Z}_n$. The minimization of e leads to

$$\begin{aligned}\underline{\mathbf{Q}} &= \underline{\mathbf{H}}_n^H(\underline{\mathbf{H}}_n\underline{\mathbf{H}}_n^H + (\mathbb{E}\{\underline{\mathbf{X}}_n\underline{\mathbf{X}}_n^H\})^{-1}\sigma_W^2)^{-1} \\ &\approx \hat{\underline{\mathbf{H}}}_p^H(\hat{\underline{\mathbf{H}}}_p\hat{\underline{\mathbf{H}}}_p^H + (\mathbb{E}\{\underline{\mathbf{X}}_p\underline{\mathbf{X}}_p^H\})^{-1}\sigma_W^2)^{-1}, \end{aligned} \quad (5)$$

where the exact frequency response should be substituted by the estimated one. Unlike ZF, the MMSE equalizer does not tend to amplify the noise, due to the contribution of the term $(\mathbb{E}\{\underline{\mathbf{X}}_p\underline{\mathbf{X}}_p^H\})^{-1}\sigma_W^2$. However, it is more complex than ZF, even if matrix inversion and multiplications involve only diagonal matrices. Moreover, similarily to LMMSE channel estimator in (3), the MMSE equalizer requires the knowledge of σ_W^2. As a consequence, the complexity and the estimation of the noise variance can be considered as the two key features of MMSE-based methods.

III. Adaptation of Estimation Methods in NB-IoT

A. Observation Over Two Slots

We consider a channel model with a coherence time at least equal to 1 ms. This assumption is reasonable for NB-IoT applications, where the UE modules are supposed to be static (*e.g.* sensors in smart cities or home automation), or slowly moving (*e.g.* machines or other industrial applications). The validity and the limit of such assumption are discussed in Section V. Based on this, the channel frequency response does not change during two consecutive slots such as illustrated in Fig. 2, with $M = 12$. For clarity purpose, but without loss of generality, we write $\underline{\mathbf{H}}_p = \underline{\mathbf{H}}$ in order to highlight the quasi-static nature of the channel. In addition, we can suppose that the same midamble $\mathbf{X}$ is transmitted in two consecutive slots (rather than using $\mathbf{X}_{p1}$ and $\mathbf{X}_{p1}$). This is because pilot values in two consecutive slots only differ by their phase, which does not affects the statistic of the observation.

Thus, we can now consider a system of linear equations:

$$\begin{cases} \mathbf{Y}_{p1} = \underline{\mathbf{H}}\mathbf{X} + \mathbf{W}_{p1} \\ \mathbf{Y}_{p2} = \underline{\mathbf{H}}\mathbf{X} + \mathbf{W}_{p2} \end{cases}, \quad (6)$$

where $p1$ and $p2$ indicates that the observation corresponds to midamble in first and second slot, respectively. It

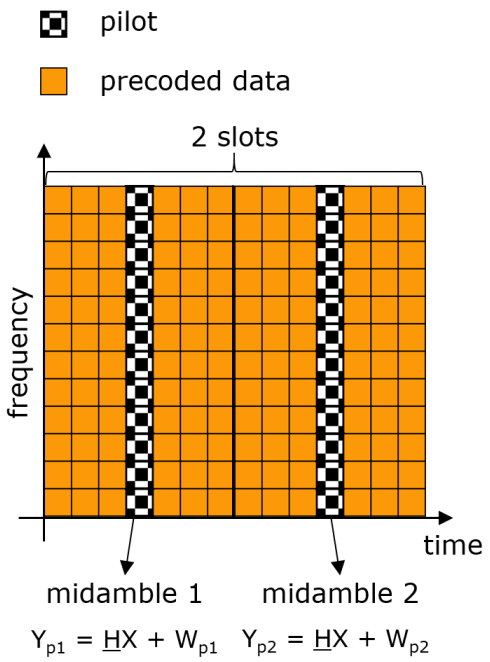

Fig. 2. Channel estimation over two slots, with $M = 12$. Channel $\mathbf{H}_p = \mathbf{H}$ is supposed constant over two slots.

can be noticed from (6) that the vectors of received pilots only differ by the additive noise. Then, it is intuitive to combine $\mathbf{Y}_{p1}$ and $\mathbf{Y}_{p2}$ to improve the channel estimation process. Therefore, to find the best combination, let us consider the likelihood function of the system (6), denoted by L. Since $\mathbf{W}_{p1}$ and $\mathbf{W}_{p2}$ are independent complex AWGN vectors, L can be written as:

$$\begin{aligned} L &= C.\exp\Big(-\frac{\|\mathbf{Y}_{p1}-\underline{\mathbf{H}}\mathbf{X}\|^2}{\sigma_W^2}\Big).\exp\Big(-\frac{\|\mathbf{Y}_{p2}-\underline{\mathbf{H}}\mathbf{X}\|^2}{\sigma_W^2}\Big) \\ &= C.\exp\Big(-\frac{\|\mathbf{Y}_{p1}\|^2+\|\mathbf{Y}_{p2}\|^2+2\|\underline{\mathbf{H}}\mathbf{X}\|^2}{\sigma_W^2} \\ &\quad + \frac{2Re\{(\underline{\mathbf{H}}\mathbf{X})^H.(\mathbf{Y}_{p1}+\mathbf{Y}_{p2})\}}{\sigma_W^2}\Big), \end{aligned} \tag{7}$$

where $C = \frac{1}{(\pi\sigma_W^2)^{2M}}$. From (7), we deduce that the maximization of L according to $\underline{\mathbf{H}}$ depends on $\mathbf{Y}_{p1}+\mathbf{Y}_{p2}$, which means that the exhaustive information of the system (6) is included in $\mathbf{Y}_{p1}+\mathbf{Y}_{p2}$. In other words, the best combination of $\mathbf{Y}_{p1}$ and $\mathbf{Y}_{p2}$ for channel estimation is the addition, and thus we can define a new observation:

$$\mathbf{Y}^+ = \frac{\mathbf{Y}_{p1}+\mathbf{Y}_{p2}}{2} = \underline{\mathbf{H}}\mathbf{X} + \frac{\mathbf{W}_{p1}+\mathbf{W}_{p2}}{2}, \tag{8}$$

to perform the channel estimation (as previously presented). It is noteworthy that over two slots, the variance of the equivalent noise in (8) is given by $\mathbb{E}\{\frac{W_{p1,m}+W_{p2,m}}{2}(\frac{W_{p1,m}+W_{p2,m}}{2})^*\} = \frac{\sigma_W^2}{2}$ for any $m = 0,1,..,M-1$, *i.e.* the noise power in $\mathbf{Y}^+$ is reduced by 3 dB compared to $\mathbf{Y}_p$. We deduce that the usage of $\mathbf{Y}^+$ instead of $\mathbf{Y}_p$ should improve the channel estimation performance.

B. Noise Variance Estimator

It has been mentioned in Section II that LMMSE estimation and MMSE equalization require the knowledge of the noise variance σ_W^2, which could limit their practical implementation. The ML estimation of the noise variance deduced from (7) leads to

$$\hat{\sigma}_W^2 = \frac{\|\mathbf{Y}_{p1}-\underline{\mathbf{H}}\mathbf{X}\|^2+\|\mathbf{Y}_{p2}-\underline{\mathbf{H}}\mathbf{X}\|^2}{2M}. \tag{9}$$

We deduce that this estimator requires the channel frequency response. Therefore, it cannot be implemented in practice. It is then interesting to suggest an efficient noise variance estimator that is independent of the channel, and that makes MMSE-based methods applicable in practice.

1) Expression of the Estimator: In addition to the improvement of the channel estimation performance by using $\mathbf{Y}^+$, we also deduce a noise variance estimator from (6). Thus, we can define a new observation denoted by $\mathbf{Y}^-$ and expressed as

$$\mathbf{Y}^- = \mathbf{Y}_{p1}-\mathbf{Y}_{p2} = \mathbf{W}_{p1}-\mathbf{W}_{p2}, \tag{10}$$

where $\mathbb{E}\{|Y_m^-|^2\} = 2\sigma_W^2$ for any $m = 0,1,..,M-1$. Then, we deduce a noise variance estimator:

$$\hat{\sigma}_W^2 = \frac{1}{2M}\sum_{m=0}^{M-1}|Y_m^-|^2. \tag{11}$$

It must be noted that, unlike $\mathbf{Y}^+$, $\mathbf{Y}^-$ does not *a priori* guarantee the optimality of the estimator (11), since the exhaustive information of the system (6) is not included in $\mathbf{Y}^-$. In fact, an *a posteriori* performance analysis of the suggested estimator shows that it does not reach the Cramer-Rao bound (CRB).

2) Performance Analysis: We straightforwardly show that the noise variance estimator is unbiased. Thus, we express the bias, denoted $B(\hat{\sigma}_W^2)$, as

$$\begin{aligned} B(\hat{\sigma}_W^2) &= \mathbb{E}\{\sigma_W^2-\hat{\sigma}_W^2\} \\ &= \sigma_W^2 - \frac{1}{2M}\sum_{m=0}^{M-1}\mathbb{E}\{|Y_m^-|^2\} = 0. \end{aligned} \tag{12}$$

In addition, we derive the variance of the estimator, denoted $V(\hat{\sigma}_W^2)$, as

$$\begin{aligned} V(\hat{\sigma}_W^2) &= \mathbb{E}\{(\sigma_W^2-\hat{\sigma}_W^2)^2\} \\ &= \mathbb{E}\{\sigma_W^4+(\hat{\sigma}_W^2)^2-2\sigma_W^2\hat{\sigma}_W^2\} \\ &= \frac{\sigma_W^4}{M}, \end{aligned} \tag{13}$$

since we have

$$\mathbb{E}\{(\hat{\sigma}_W^2)^2\} = \mathbb{E}\Big\{\frac{1}{4M^2}\Big(\sum_{m=0}^{M-1}|Y_m^-|^2\Big)^2\Big\}$$
$$= \frac{1}{4M^2}\sum_{k=0}^{M-1} 8\sigma_W^4 + \frac{1}{4M^2}\sum_{m=0}^{M-1}\sum_{\substack{n=0\\n\neq m}}^{M-1} 4\sigma_W^4$$
$$= \frac{2}{M}\sigma_W^4 + \frac{M-1}{M}\sigma_W^4. \quad (14)$$

We can now show that the variance of the estimator is equal to its CRB, which means that the suggested noise variance is efficient. In appendix, we first show that the estimation of the noise variance is independent of the estimation of the M channel frequency coefficients. Mathematically, this is highlighted by the fact that the Fisher information matrix is block diagonal, where one block is the scalar corresponding to the noise variance. Then, the CRB of the noise variance is obtained through the inversion of a scalar, and does not require the inversion of the whole Fisher information matrix. Accordingly, the CRB of the noise variance estimator, denoted by $CRB(\hat{\sigma}_W^2)$, is given by the scalar:

$$CRB(\hat{\sigma}_W^2) = -\mathbb{E}\Big\{\frac{\partial^2}{\partial(\sigma_W^2)^2}\ln(L)\Big\}^{-1} = \frac{\sigma_W^4}{2M}, \quad (15)$$

where L is defined in (7). The detailed development are provided in Appendix. We verify that $V(\hat{\sigma}_W^2) > CRB(\hat{\sigma}_W^2)$, which highlights the non-optimality of the suggested estimator. However, it must be reminded that this estimator is implementable in practice, since it does not require any knowledge of the channel, contrarily to ML noise variance estimator in (9).

IV. Simulations Results

As simulations parameters, we consider a NB-IoT uplink SC-FDMA signal with $M = 12$ subcarriers of 15 kHz spacing, and carrying QPSK data elements (according to [1], no higher order constellation is allowed in NB-IoT). The signal is transmitted through a typical urban channel such as described in TR 25.943 [15]. It is composed of 20 paths, with a maximum delay spread of 2.14 μs. The different techniques presented for estimation and equalization are compared in terms of bit error rate (BER) and normalized MSE (NMSE), defined as $NMSE = \frac{\mathbb{E}\{\|\hat{H}_m - H_m\|^2\}}{\mathbb{E}\{\|H_m\|^2\}}$. In our case, we approximate the expectation by an average over 1000 simulation runs.

A. BER Performance Over One Slot

In Fig. 3, we start by comparing LS and LMMSE estimation combined to ZF and MMSE equalization techniques in terms of BER versus SNR (dB) over one slot. To apply LMMSE and MMSE, we suppose that the noise variance is known at the receiver. The curve corresponding to perfect channel estimation (denoted by perfect chest.) is considered as a lowest bound reference (an MMSE equalization is used here).

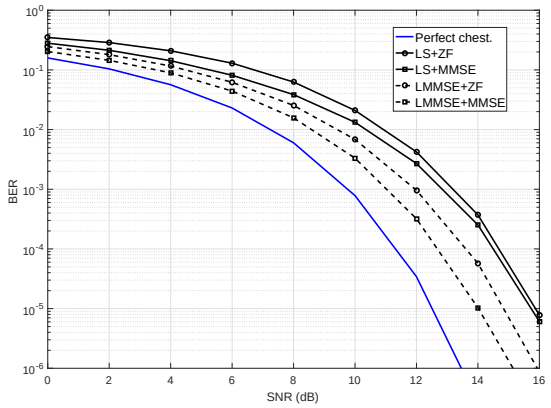

Fig. 3. BER performance vs SNR of LS, LMMSE, ZF, and MMSE over 1 slot.

If we denote the four possible combinations LS+ZF (A), LS+MMSE (B), LMMSE+ZF (C), LMMSE+MMSE (D), then we can observe that, for any SNR, the BER performance is (A)≤(B)≤(C)≤(D). More precisely, we notice that, at BER=10^{-4}, a performance gain of 1.1 dB is achieved by LMMSE+ZF compared to LS+ZF, and a performance gain of 1.8 dB is achieved by LMMSE+MMSE compared to LS+MMSE. This result highlights the smoothing effect of LMMSE in comparison with LS channel estimate, which reduces the noise distortion.

Moreover, Fig. 3 shows that the better the channel estimate, the better the MMSE equalizer compared with ZF. In fact, at BER=10^{-4}, the SNR gain is of 0.2 dB using LS estimator, and 0.9 dB using LMMSE estimator. This is due to two reasons, the first one is that we use the channel estimates instead of the exact channel frequency response in (4) and (5). The second one is that ZF tends to amplify the noise compared with MMSE, in particular in presence of channel estimation errors.

Another observation is that perfect channel estimation outperforms LMMSE+MMSE of more than 1 dB. However, we can notice in papers such as [11] that LMMSE is very close to perfect estimation. The reason is that we are using SC-FDMA contrarily to [11] where OFDM is considered. In OFDM, an error of estimation and equalization only induce self-interference, whereas in SC-FDMA, such errors also induce intercarrier interference due to the transform decoding stage.

B. Performance Over Two Slots

In the following, we focus on the adaptation of estimation methods to NB-IoT over 2 slots. Thus, to show the advantage of estimating over 2 slots rather than 1 slot, we show in Fig. 4 the NMSE of LS and LMMSE estimators versus SNR (dB). Note that LMMSE is performed with the

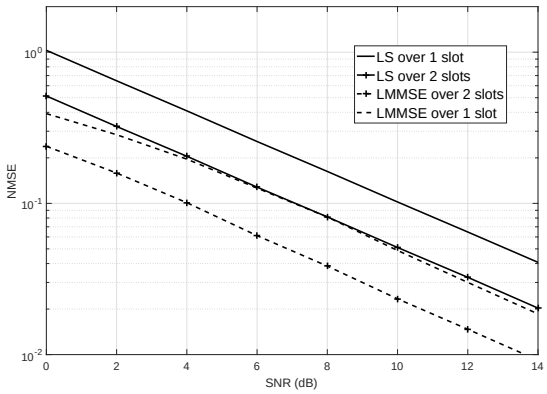

Fig. 4. Channel estimation NMSE vs SNR (dB) for LS and LMMSE. Comparison of estimation over 1 slot and 2 slots.

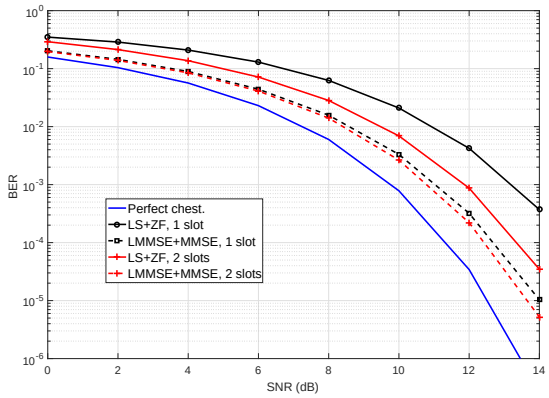

Fig. 5. BER performance vs SNR (dB) of LS+ZF and LMMSE+MMSE over 1 slot and 2 slots.

exact noise variance. It can be observed that a gain of 3 dB is achieved using 2 slots compared with 1 slot for both LS and LMMSE. This is consistent with the theoretical results deduced from (8). Moreover, we can notice that the performance of LMMSE over one slot coincides with the NMSE of LS over two slots. We can then concludes that the smoothing effect of LMMSE also reduces the noise variance by half and thus improves the BER performance as observed in Fig. 3.

In Fig. 5, we compare the BER versus SNR (dB) of the worst combination (LS+ZF) and the best combination (LMMSE+MMSE) over 1 and 2 slots. We observe that at BER=10^{-3} the LS+ZF methods over 2 slots achieve a SNR gain of 1.4 dB compared to the same methods performed over 1 slot. However, the gain is only 0.3 dB for LMMSE+MMSE methods. This result shows that the estimation over 2 slots is more beneficial for low-performance methods such as LS+ZF, whereas LMMSE+MMSE seems to reach a BER lower bound. Once again, this limit can be explained by the modulation scheme, which is sensitive to channel estimation errors, since these errors induce intercarrier interference.

C. Performance of the Noise Variance Estimator

Further series of simulations investigate the performance of the suggested noise variance estimation and its effects on LMMSE and MMSE methods. Fig. 6 depicts the MSE of the noise variance estimator in (11) versus SNR (dB), the ML in (9), and the corresponding CRB. It can be observed that the MSE of ML matches the CRB, whereas the MSE of the proposed estimator is twice the CRB, such as predicted in (13) and (15). However, we will show that the noise variance estimator is efficient, even for low subcarriers number, and can then be used to feed LMMSE and MMSE techniques.

To show the performance of the proposed noise variance estimator when used in LMMSE and MMSE, we plot in Fig. 7 the BER versus SNR (dB) of LMMSE+MMSE

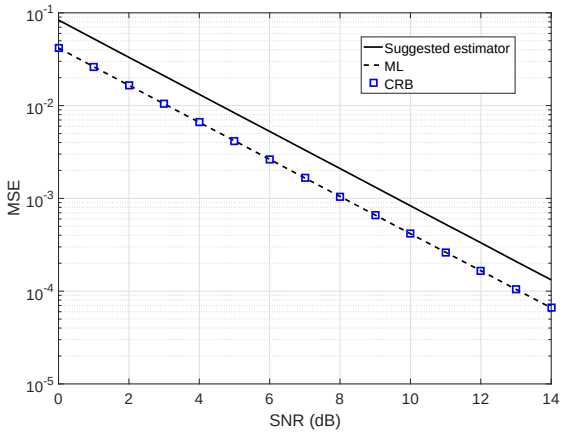

Fig. 6. MSE of noise variance estimation versus SNR (dB). Comparison of theoretical CRB and simulation.

using exact noise variance and estimated noise variance. It can be noticed that the two curves match, and thus we conclude that both LMMSE and MMSE can be used in practice, since the noise variance is efficiently estimated. However, the only remaining limitation is the complexity of these methods, which is left to be discussed in next section.

V. Discussion

A. Complexity Analysis

In this section, we analyze the complexity of the presented methods through the number of complex multiplications. From (2), we deduce that the complexity of LS is M multiplications. For LMMSE, we consider that the known approximated channel covariance matrix $\underline{\tilde{\mathbf{R}}}_H$ is used in (3). To obtain $\underline{\tilde{\mathbf{R}}}_H$, a constant channel gain delay profile is assumed. Thus, the complexity of matrix inversion and multiplication is reduced from $2M^3$ to M^2 (see [11] for details). Moreover, it must be noticed that pilots have a constant modulus, thus $(\underline{\mathbf{X}}_p\underline{\mathbf{X}}_p^H)^{-1}$ is a

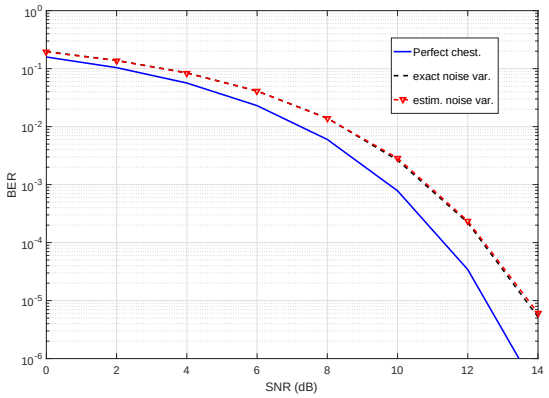

Fig. 7. BER performance versus SNR (dB) of LMMSE+MMSE using exact noise variance and estimated noise variance.

diagonal matrix. This makes the complexity of LMMSE using $\underline{\tilde{\mathbf{R}}}_H$ is equal to M^2+2M, where $2M$ corresponds to the complexity of the estimation of noise variance using (11) combined with that of the LS estimator.

Despite the number of multiplications grows by the square of M, the complexity of such technique is tightly related to the technology being used. Therefore, in NB-IoT $M \leq 12$, the relative complexity of LMMSE compared with LS is low (168 operations), and thus it is practically implementable in eNBs. For instance, M in digital video broadcasting-terrestrial 2 (DVB-T2) is up to 32K. In this respect, LMMSE requires a high computation cost for such technology (about 10^9 operations). To summarize, it is possible to take advantage of the low number of subcarriers in NB-IoT to implement LMMSE in eNBs, in particular since it significantly improves the performance of the receiver.

For equalization, ZF involves M operations, whereas MMSE requires $4M$ multiplications: M for noise variance estimation, M for $\underline{\hat{\mathbf{H}}}_p\underline{\hat{\mathbf{H}}}_p^H$, M for the inversion, and M for the multiplication by $\underline{\hat{\mathbf{H}}}_p$. We conclude that MMSE is slightly more complex than ZF, but it is very suitable to be used in NB-IoT eNBs.

B. Coherence Time Validity

The coherence time of a channel is defined as the duration over which the propagation channel can be considered as not varying. Different models are given in [16], according to more or less restrictive conditions on the term "not varying". In this paper, we assume that the channel is constant over at least a subframe (*i.e.* 1 ms). Then the coherence time T_c can be expressed as

$$10^{-3} \leq T_c = \frac{9}{16\pi f_D}, \tag{16}$$

where $f_D = \frac{v.f_0}{c}$ is the Doppler frequency, with v the relative velocity between transmitter and receiver, f_0 the central frequency of the signal, and c the light speed. If f_0 is of order of 1 GHz, then the speed v corresponding to 1 ms coherence time is upper bounded as $v \leq 53.7$ m.s^{-1}, or 190 km.h^{-1}. We conclude that the considered assumption holds for a mobility of about a hundred kilometers per hour, which validates the developments in Section III.

VI. Conclusion

In this paper, we addressed the uplink estimation and equalization techniques used in LTE system and their possible adaptation to NB-IoT system. To this end, we briefly presented how NB-IoT system frame is inherited from the LTE one, and showed the main differences between their uplink signals. Two estimation (LS and LMMSE) and two equalization (ZF, MMSE) techniques were considered. The adaptation of these techniques was demonstrated by taking into account the characteristics of the NB-IoT uplink signal. Furthermore, a noise variance estimator, which uses observations over two slots, has been proposed. Simulations were performed for all the combinations of the estimation and equalization techniques. Results revealed that the use of the LMMSE estimator with MMSE equalization techniques lead to the best performance, in particular when the estimation is done over 2 slots. In contrast, the LMMSE estimation combined to MMSE equalization lead to higher computation complexity (but it is tightly related to the number of subcarriers). However, the complexity analysis showed that since the NB-IoT system has a bandwidth of only 180 KHz (12 subcarriers of 15 KHz), the LMMSE estimation combined to MMSE can be the best to be used for such system. In future works, we will extend the analysis to the single carrier modulation mode, including 15 kHz and 3.75 kHz subcarrier spacing.

Appendix

The appendix aims to prove the CRB given in (15) for noise variance estimation. We base our proof on the CRB analysis for complex parameters as in [17], but we extend the developments in [17] to the case of non-holomorphic functions by using Wirtinger's derivative [18], [19] instead of usual complex derivative. Let us denote $\mathbf{T}$ the vector of the complex parameters of the system (6), *i.e.* $\mathbf{T} = [H_0, H_0^*, H_1, H_1^*, .., H_{M-1}, H_{M-1}^*, \sigma_W^2]$, where H_m, $m = 0, 1, .., M-1$, are the channel frequency response coefficients. We first show that the channel and the noise variance can be estimated independently by proving that $\mathbb{E}\Big\{\frac{\partial}{\partial H_m^* \partial} \ln(L)^* \frac{\partial}{\partial \sigma_W^2} \ln(L)\Big\} = 0$, for any $m = 0, 1, .., M-1$. In that case, the Fisher information matrix $\underline{\mathbf{K}}$, whose elements at u-th row and v-th column $(u, v = 0, 1, .., M)$ are defined (see (11) in [17]) by

$$K_{u,v} = \mathbb{E}\Big\{\frac{\partial}{\partial T_u^*} \ln(L)^* \frac{\partial}{\partial T_v} \ln(L)\Big\}, \tag{17}$$

is block diagonal, where one block corresponds to the channel, and the other block is the scalar corresponding to the noise variance. Thus, the CRB of the noise variance

is only defined by a scalar given in (15), and it is not mandatory to calculate the whole matrix $\underline{\mathbf{K}}$.

It must be noted that the following developments involve non-holomorphic functions. Therefore, Wirtinger's derivative [18], [19] is used instead of usual complex derivative. Thus, the log-likelihood function $\ln(L)$ can be developed as follows:

$$\ln(L) = \ln(C) - \frac{1}{\sigma_W^2}\Big[\sum_{m=0}^{M-1} |Y_{p1,m}|^2 + |Y_{p2,m}|^2 + 2|H_m X_m|^2 - 2Re\big\{H_m^* X_m^* (Y_{p1,m} + Y_{p2,m})\big\}\Big]. \quad (18)$$

Then, since for $z \in \mathbb{C}$, $Re\{z\} = \frac{z+z^*}{2}$, and $\frac{\partial z^*}{\partial z} = 0$ (Wirtinger's derivative), for any $m = 0, 1, .., M-1$, we have:

$$\frac{\partial}{\partial H_m^*} \ln(L)^* = -\frac{2H_m|X_m|^2 - X_m^*(Y_{p1,m} + Y_{p2,m})}{\sigma_W^2}, \quad (19)$$

and

$$\frac{\partial}{\partial \sigma_W^2} \ln(L) = \frac{-2M}{\sigma_W^2} + \frac{\sum_{m=0}^{M-1} |Y_{p1,m} - H_m X_m|^2}{\sigma_W^4} + \frac{\sum_{m=0}^{M-1} |Y_{p2,m} - H_m X_m|^2}{\sigma_W^4}. \quad (20)$$

It can be noted that $\mathbb{E}\{X_m(Y_{p1,m}+Y_{p2,m})^*\} = 2H_m^*|X_m|^2$, since $\mathbb{E}\{W_{p1,m}\} = \mathbb{E}\{W_{p2,m}\} = 0$. After some mathematical developments that are not detailed in this paper, it follows that $\mathbb{E}\Big\{\frac{\partial}{\partial H_m^*} \ln(L)^* \frac{\partial}{\partial \sigma_W^2} \ln(L)\Big\} = 0$. Furthermore, it is straightforward that the regularity condition holds. As consequence, we can focus on $-\mathbb{E}\Big\{\frac{\partial^2}{\partial(\sigma_W^2)^2} \ln(L)\Big\}$ to calculate the CRB of the noise variance estimator:

$$\frac{\partial^2}{\partial(\sigma_W^2)^2} \ln(L) = \frac{2M}{\sigma_W^4} - \frac{2}{\sigma_W^6}\Big[\sum_{m=0}^{M-1} |Y_{p1,m} - H_m X_m|^2 + |Y_{p2,m} - H_m X_m|^2\Big]. \quad (21)$$

We have

$$\mathbb{E}\{|Y_{pi,m} - H_m X_m|^2\} = \sigma_W^2,$$

for $i = 1, 2$, hence we deduce the CRB as

$$CRB(\hat{\sigma}_W^2) = -\mathbb{E}\Big\{\frac{\partial^2}{\partial(\sigma_W^2)^2} \ln(L)\Big\}^{-1} = \frac{\sigma_W^4}{2M}, \quad (22)$$

which concludes the proof.

References

[1] 3GPP, "3GPP TS 36.211, Physical channels and modulation (Release 14)," 3GPP, Tech. Rep., March 2017.

[2] R. Ratasuk, N. Mangalvedhe, Y. Zhang, and J.-P. Robert, M. Koskinen, "Overview of Narrowband IoT in LTE Rel-13," in *proc. of CSCN'16*, Berlin, Germany, November 2016, pp. 1 – 7.

[3] J. Schlienz and D. Raddino, "Narrowband Internet of Things - Whitepaper," Rohde & Schwarz, Tech. Rep., 2016.

[4] Y.-P. E. Wang, X. Lin, A. Adhikary, A. Grövlen, Y. Sui, J. Blankenship, Y. Bergman, and H. S. Razaghi, "A Primer on 3GPP Narrowband Internet of Things," *IEEE Communications Magazine*, vol. 55, no. 3, pp. 117 – 123, March 2017.

[5] Ericson, "Internet of Things forecast." [Online]. Available: https://www.ericsson.com/en/mobility-report/internet-of-things-forecast

[6] S. Pratschner, S. Schwarz, and M. Rupp, "Single-user and multi-user MIMO channel estimation for LTE-Advanced uplink," in *proc. of ICC'17*, Paris, France, May 2017, pp. 1 – 6.

[7] D. Li and K. Feng, "Fast Time-Varying Channel Estimation Method for LTE SC-FDMA System," in *proc. of ICASSP'14*, Florence, Italy, May 2014, pp. 1 – 5.

[8] S. Coleri, M. Ergen, A. Puri, and A. Bahai, "A study of channel estimation in ofdm systems," in *Vehicular Technology Conference*, vol. 2, september 2002, pp. 894–898.

[9] M. K. Ozdemir and H. Arslan, "Channel estimation for wireless OFDM systems," *IEEE Communications Surveys and Tutorials*, vol. 9, no. 2 (2nd Quarter), pp. 18 – 48, July 2007.

[10] Y. Liu, Z. Tan, H. Hu, L. J. Cimini, and G. Y. Li, "Channel estimation for OFDM," *IEEE Communications Surveys and Tutorials*, vol. 16, no. 4 (4th Quarter), pp. 1891 – 1908, May 2014.

[11] V. Savaux and Y. Louët, "LMMSE channel estimation in OFDM context: a review," *IET Signal Processing*, vol. 11, no. 2, pp. 123 – 134, April 2017.

[12] O. Edfors, M. Sandell, J.-J. van de Beek, S. K. Wilson, and P. O. Börjesson, "OFDM Channel Estimation by Singular Value Decomposition," *IEEE Trans. on Communications*, vol. 46, no. 7, pp. 931 – 939, July 1998.

[13] V. Savaux, Y. Louët, M. Djoko-Kouam, and A. Skrzypczak, "Minimum mean-square-error expression of LMMSE channel estimation in SISO OFDM systems," *IET Electronics Letters*, vol. 49, no. 18, pp. 1152 – 1154, August 2013.

[14] O. Edfors, M. Sandell, J.-J. Van de Beek, S. K. Wilson, and P. O. Borjesson, "OFDM channel estimation by singular value decomposition," in *proc. of VTC'96*, Atlanta, GA, USA, May 1996, pp. 923 – 927.

[15] 3GPP, "3GPP TR 25.943: 'Universal Mobile Telecommunications System (UMTS); Deployment aspects (Release 9)'," 3GPP, Tech. Rep., February 2010.

[16] B. Sklar, "Rayleigh fading channels in mobile digital communication systems .I. Characterization," *IEEE Communications Magazine*, vol. 35, no. 7, pp. 90 – 100, July 1997.

[17] A. Van den Bos, "A Cramér-Rao Lower Bound for Complex Parameters," *IEEE Transactions on Signal Processing*, vol. 42, no. 10, p. 2859, October 1994.

[18] P. Bouboulis, "WirtingerŠs Calculus in general Hilbert Spaces," *ArXiv*, vol. rXiv:1005.5170v1, pp. 1 – 27, May 2010.

[19] T. Adali and P. J. Schreier, "Optimization and Estimation of Complex-Valued Signals: Theory and applications in filtering and blind source separation," *IEEE Signal Processing Magazine*, vol. 31, no. 5, pp. 112 – 128, September 2014.